

Effects of hole-injection through side-walls of large V-pits on efficiency droop in Ⅲ-nitride LEDs

Dong-Yan Zhang(张东炎), Jie Zhan(张洁), Xiao-Feng Liu(刘晓峰), Sha-Sha Chen(陈沙沙), Hui-Wen Li(李慧文), Ming-Qing Liu(刘明庆), Da-Qian Ye(叶大千), Du-Xiang Wang(王笃祥)

Citation: Chin. Phys. B . 2019, 28(4): 048501. **doi:** 10.1088/1674-1056/28/4/048501
Journal homepage: http://cpb.iphy.ac.cn; http://iopscience.iop.org/cpb

What follows is a list of articles you may be interested in

Improved carrier injection and confinement in InGaN light-emitting diodes containing GaN/AlGaN/GaN triangular barriers

Li-Wen Cheng(程立文), Jian Ma(马剑), Chang-Rui Cao(曹常锐), Zuo-Zheng Xu(徐作政), Tian Lan(兰天), Jin-Peng Yang(杨金彭), Hai-Tao Chen(陈海涛), Hong-Yan Yu(于洪岩), Shu-Dong Wu(吴曙东), Shun Yao(尧舜), Xiang-Hua Zeng(曾祥华), Zai-Quan Xu(徐仔全)

Chin. Phys. B . 2018, 27(8): 088504. **doi:** 10.1088/1674-1056/27/8/088504

Enhanced performances of InGaN/GaN-based blue light-emitting diode with InGaN/AlInGaN superlattice electron blocking layer

Zhuo Xiang-Jing, Zhang Jun, Li Dan-Wei, Yi Han-Xiang, Ren Zhi-Wei, Tong Jin-Hui, Wang Xing-Fu, Chen Xin, Zhao Bi-Jun, Wang Wei-Li, Li Shu-Ti
Chin. Phys. B . 2014, 23(6): 068502. **doi:** 10.1088/1674-1056/23/6/068502

A GaN–AlGaN–InGaN last quantum barrier in an InGaN/GaN multiple-quantum-well blue LED

Yang Bin, Guo Zhi-You, Xie Nan, Zhang Pan-Jun, Li Jing, Li Fang-Zheng, Lin Hong, Zheng Huan, Cai Jin-Xin
Chin. Phys. B . 2014, 23(4): 048502. **doi:** 10.1088/1674-1056/23/4/048502

Efficiency enhancement of an InGaN light-emitting diode with a p-AlGaN/GaN superlattice last quantum barrier

Xiong Jian-Yong, Zhao Fang, Fan Guang-Han, Xu Yi-Qin, Liu Xiao-Ping, Song Jing-Jing, Ding Bin-Bin, Zhang Tao, Zheng Shu-Wen
Chin. Phys. B . 2013, 22(11): 118504. **doi:** 10.1088/1674-1056/22/11/118504

Performance enhancement of an InGaN light-emitting diode with an AlGaN/InGaN superlattice electron-blocking layer

Xiong Jian-Yong, Xu Yi-Qin, Zhao Fang, Song Jing-Jing, Ding Bin-Bin, Zheng Shu-Wen, Zhang Tao, Fan Guang-Han
Chin. Phys. B . 2013, 22(10): 108505. **doi:** 10.1088/1674-1056/22/10/108505

Effects of hole-injection through side-walls of large V-pits on efficiency droop in III–nitride LEDs*

Dong-Yan Zhang(张东炎)[1,2,†], Jie Zhang(张洁)[3], Xiao-Feng Liu(刘晓峰)[1,2], Sha-Sha Chen(陈沙沙)[1,2], Hui-Wen Li(李慧文)[1,2], Ming-Qing Liu(刘明庆)[1,2], Da-Qian Ye(叶大千)[1,2], and Du-Xiang Wang(王笃祥)[1,2]

[1] *Tianjin San'an Optoelectronics Co., Ltd, No. 20 Haitainan Road, Huayuan New Technology Industry Development Area, Tianjin 300384, China*
[2] *The Key Laboratory of Semiconductor LED Chip of Tianjin, No. 20 Haitainan Road, Huayuan New Technology Industry Development Area, Tianjin 300384, China*
[3] *Xiamen San'an Optoelectronics Technology Co., Ltd, No. 1721-1725, Luling Road, Xiamen 361009, China*

(Received 9 October 2018; revised manuscript received 11 February 2019; published online 5 March 2019)

Although the solid-state lighting market is growing rapidly, it is still difficult to obtain ultra-high brightness white light emitting diodes (LEDs). V-pits are inevitably introduced during the metalorganic chemical vapor deposition (MOCVD) growth of multiple quantum wells (MQWs) in III–nitride LEDs, and thus affecting the carrier dynamics of the LEDs. Specifically designed structures are fabricated to study the influence of the V-pits on the hole transportation and efficiency droop, and double quantum wells (QWs) are used to monitor the transportation and distribution of holes based on their emission intensity. It is found that when compared with the planar QWs, the injection of holes into the QWs through the side walls of the V-pits changes the distribution of holes among the MQWs. This results in a higher probability of hole injection into the middle QWs and enhanced emission therein, and, consequently, a lower efficiency droop.

Keywords: V-pits, efficiency droop, side-wall, injection

PACS: 85.30.–z, 66.70.Df, 72.20.–i **DOI:** 10.1088/1674-1056/28/4/048501

1. Introduction

To dominate the solid-state lighting (SSL) market, applications of group III–nitride InGaN/GaN light emitting diodes (LEDs) with higher efficiency at high injection current density must prevail.[1–4] However, one of the most significant and enduring challenges facing high-power GaN-based LEDs is the efficiency droop, which is the decrease in external quantum efficiency (EQE) of LEDs with the increasing driving current. While the real culprit of droop is still under debate, and nearly all of the investigations attributed the efficiency droop to Auger recombination, defect related mechanism and electron leakage.[5–8] But all of the analyses focused on the LEDs without V-pits, which were inevitably formed during the MOCVD growth of quantum wells (QWs) in the real III–nitride LEDs.[9,10] Actually, due to the lack of proper substrates, commercial blue and green LEDs are conventionally grown directly on sapphire substrates, despite the large mismatch both in lattice and in thermal expansion. A high density of dislocations was usually produced, acting as non-radiative recombination centers and even leading to the formation of V-shaped pits (V-pits) with six {10-11} planes.[11] Typically the density of V-pits was higher than $1 \times 10^7/\text{cm}^2$, and the formation of V-pits was triggered by the threading dislocations (TDs).[12] As a kind of large-size defect that usually penetrate into the MQW active region of an LED, V-pits definitely affect the carrier dynamics and the efficiency of III–nitride LEDs. So, it is critical to understand the relationships between V-pits and droop properties to improve the efficiency of III–nitride blue and green LEDs at large driving current densities.

Recently, intensive attention has been paid to establishing a connection between V-pits and the optical or electrical properties of LEDs. The size of the V-pits could be enlarged by using an InGaN/GaN superlattice (SL) inserted beneath the MQWs to improve the electroluminescence (EL) intensity and internal quantum efficiency (IQE).[13,14] Kim *et al.* reported that the reverse leakage current of InGaN LEDs with larger V-pits was significantly reduced by several orders of magnitude: from 1.8 mA down to 3.84 nA at 30 V.[15] Some experiments have pointed that if the density and size of V-pits increased as the period number of QWs increases from three to five, then the LEDs would suffer a larger leakage current and deteriorated EL characteristics.[16] However, our simulation results show that V-pits could screen dislocations and promote hole injection into the MQWs.[12,13,17] Based on K. P simulations, it was found that higher energy barrier around V-pits in InGaN QWs could effectively suppress the non-radiative recombination at TDs, and thus alleviate the efficiency droop.[18] By using monolithic dual-wavelength MQWs and measuring the EL spectra at different current densities, the depth of hole in-

*Project supported by the National Key Research and Development Project of China (Grant No. 2017YFB0403303) and the Key Technologies Research and Development Program of Tianjin, China (Grant Nos. 18YFZCGX00760 and 18YFZCGX00400).

†Corresponding author. E-mail: dyzhang2012@sanan-e.com

© 2019 Chinese Physical Society and IOP Publishing Ltd

jection was estimated.[19] However, these experiments were based on differently sized V-pits and the longer wavelength photoluminescence excited by the shorter wavelength emission from other QWs was not considered. There are few reports on the distribution of carriers in the LEDs with large size of V-pits, and little experimental evidence to support these theoretical conclusions.

In this work, the effects of V-pits on the efficiency droop of III–nitride LEDs are investigated by using specifically designed LED structures. The carrier distributions under different current densities and efficiency droop were investigated by means of the monitor double QWs (DQWs) at different locations. Our results show that the distribution of injected holes is changed by the existence of V-pits as compared with the scenario of the planar LEDs. The efficiency droop is mitigated due to the large-size of the V-pits.

2. Experiments

LED samples were grown on c-plane patterned sapphire substrates (PSS) by a high-speed, rotating-disk MOCVD system (Veeco K465i). The structures of samples A, B, and C are the same but the locations of the monitor DQWs are different. Starting from sapphire substrates, the LED structures consist of a 3-μm thick nominally un-doped GaN layer, a 2-μm thick Si-doped n-type GaN layer with a concentration of $\sim 1\times10^{19}$/cm^3. This was followed by the pre-strain layers with three periods of $\sim$ 1.5-nm InGaN quantum wells and $\sim$ 60-nm GaN barriers. Six-pairs of $\sim$ 1.5-nm $In_{0.14}Ga_{0.86}N$/$\sim$ 5-nm GaN superlattice (SLs) were used to enlarge the V-pits,[9] and then 10 periods of $\sim$ 3-nm thick InGaN wells and $\sim$ 10-nm thick GaN barriers as the active region, with eight QWs of 450-nm emission and monitor DQWs of 475-nm emission, as schematically shown in Fig. 1(a), subsequently 10-period $Al_{0.20}Ga_{0.80}N$/GaN superlattice electron blocking layer (EBL) with a total thickness of 24 nm on the top of MQWs, finally, $\sim$ 100-nm thick Mg-doped p-GaN with a nominal hole density of 3×10^{17}/cm^3–7×10^{17}/cm^3 was grown to complete the LED structures. The monitor DQWs were located at the bottom, the middle, and the top of the active region, in samples A, B, and C, respectively. By replacing the QWs of 450-nm emission of samples A, B, and C with GaN of the same thickness, samples D, E, and F were grown, respectively, while keeping the thickness of all the other corresponding layers unchanged, as shown in Fig. 1(b). To keep the same well depth as that of commercial blue LEDs, the emission wavelengths of DQWs were changed into 450 nm in samples D, E, and F. These devices were designed in lateral injection configuration with a chip dimension of 0.84 mm×0.41 mm with Ti/Al/Ti/Au n-type contacts and Ni/Au p-type contacts. The surface morphology for each epitaxial structure was characterized by Dimension 3100 atomic force microscope (AFM) system in tapping mode. The crystalline structure of the V-pits in sample A was evaluated by transmission electron microscopy (TEM).

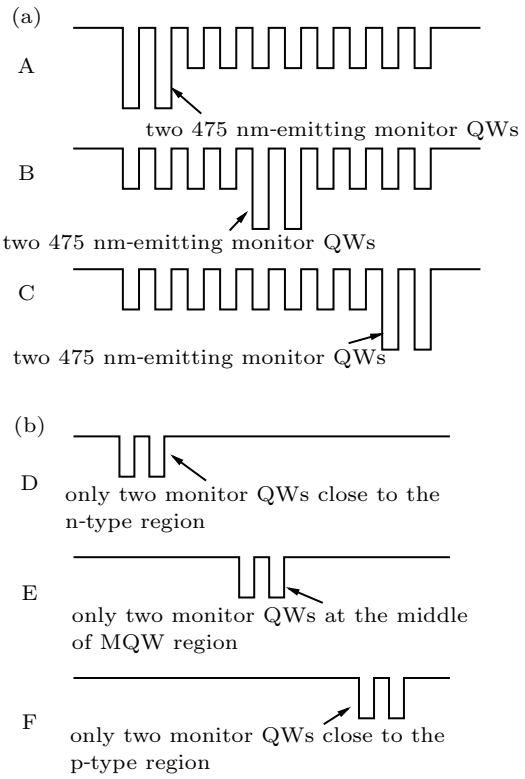


Fig. 1. Schematic conduction band diagrams for MQWs of 6 samples.

3. Results and discussion

To evaluate the effect of V-pits on the efficiency droop, DQWs of 475-nm emission are used to monitor the carrier distribution among the QWs in the LEDs, as shown in Fig. 1(a). Particularly under high driving current condition, the carrier transport behaviors in GaN/InGaN MQW LEDs can be investigated. Figure 2 shows the TEM and AFM image of Sample A, and the morphologies and shapes of V-pits in all the other samples are similar (not shown here). For the pre-strain layer and SL technology, the growth condition is optimized to achieve a white light efficiency of higher than 200 lm/W. The V-pits at position of top QW have an opening diameter of 200 nm–300 nm as shown by the cross-sectional TEM image in Fig. 2(a). Most of the V-pits start at the interface between InGaN and GaN in the pre-strain layers due to the lattice mismatch, going through the whole MQW-region. Each pit contains a threading dislocation penetrating through the apex. Thinner pairs of InGaN QWs and GaN quantum barriers (QBs) covering the side wall of V-pits can be clearly observed from the TEM image. The density of V-pits is about 2.5×10^8/cm^2 calculated based on the AFM image shown in Fig. 2(b). For the growth of a full LED structure, the large

V-pits are filled with the EBL and p-GaN material to obtain a planarized surface by using a low growth rate technology.

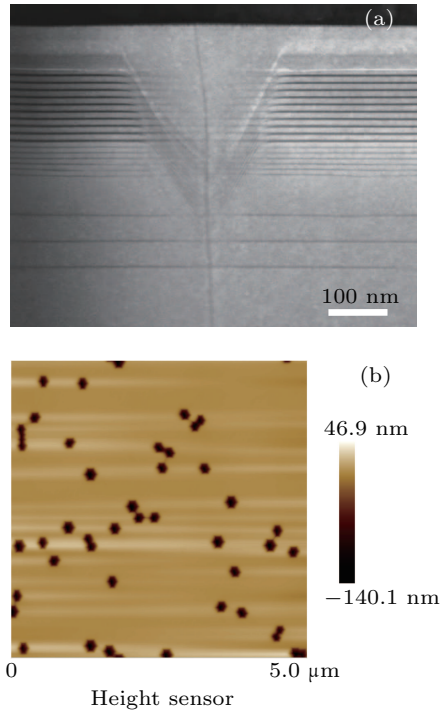


Fig. 2. Cross-sectional TEM image (a) and surface AFM-image (b) of sample A.

EL spectra for samples A, B, and C at driving current densities of 25, 60, and 100 A/cm^2 are given in Figs. 3(a)–3(c). The 450-nm and 475-nm peak can be observed simultaneously in each spectrum. All the spectra are normalized by the intensities of the corresponding 450-nm peak. It can be seen that the EL at 475 nm from the monitor DQWs is even stronger than that at 450 nm for sample B as shown in Fig. 3(a), although there are eight 450-nm QWs, which is four times of 475-nm QWs in our samples. The diffusion length of holes in MQW region is very short due to the lower hole mobility ($\sim$ 10 cm$^2\cdot$V$^{-1}\cdot$s^{-1}) than the electron mobility ($\sim$ 200 cm$^2\cdot$V$^{-1}\cdot$s^{-1}).[20] The EL intensity of each QW in the samples largely depends on the distribution of holes among the QWs. The stronger 475-nm emission from sample B than those from samples A and C at low driving current density of 25 A/cm^2 indicates that the holes are preferentially distributed in the DQW in the middle part of the active region (5th and 6th QWs from either bottom or top) and recombine with electrons there. At the same time, the relative intensity of 475-nm peak of sample B is also higher than those of samples A and C at higher driving current densities as shown in Figs. 3(b) and 3(c). This implies the higher probability of injection of holes into the *c*-plane 5th and 6th QWs from the side-wall of V-pits in a range from 25 A/cm^2 to 100 A/cm^2. The hole injection through side-walls of V-pits is schematically shown in Fig. 4(a), together with the vertical downward injection. As mentioned earlier, V-pits are filled with the EBL and p-GaN materials, holes inside the V-pits can be injected into the QWs in the middle part of the active region more easily though the side-wall due to a short distance between the p-GaN and QWs as shown by the blue arrow. Figure 4(b) shows the relative intensity of 475-nm peak varying with driving current density. It can be seen that the relative intensity decreases with driving current density increasing for samples B and C, indicating that the hole distribution among the QWs changes as the current density increases. The efficiency droop of 475-nm emission is even worse than that of the 450 nm. However, it is noted that the relative intensity of 475 nm in sample A increases as the driving current density increases. This implies that the peak of the hole distribution shifts even further to the n-GaN side.

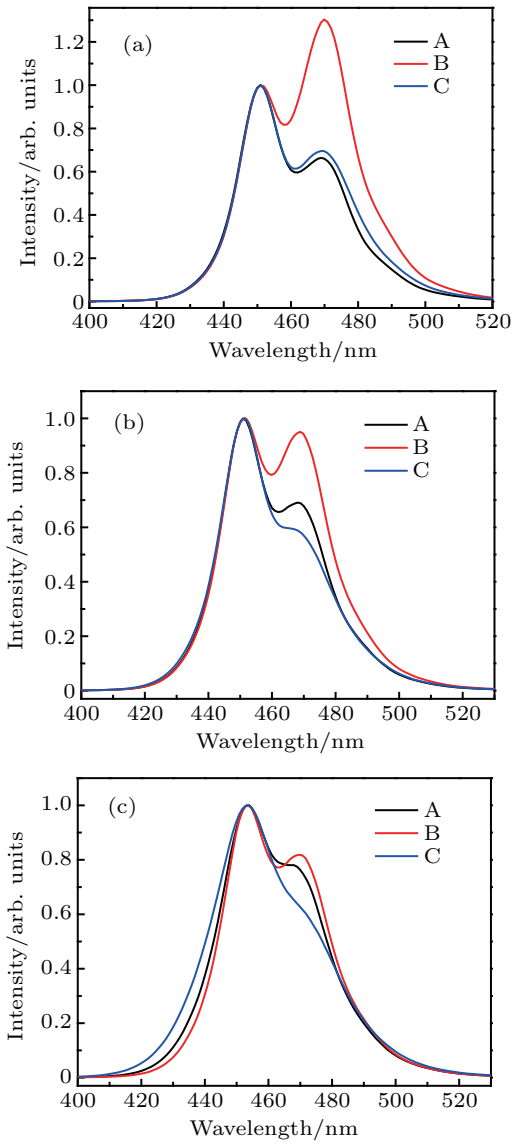


Fig. 3. (a) EL spectra of samples A, B, and C at driving current densities of (a) 25 A/cm^2, (b) 60 A/cm^2, and (c) 100 A/cm^2.

The EL spectra at different driving current densities are plotted in Fig. 5 for samples A, B, and C. The blue-shift of EL peak with the variation of driving current density is a common phenomenon in III–nitride blue and green LEDs, which results from the quantum-confined Stark effect (QCSE),[21] due

to the piezoelectric field in InGaN/GaN MQW active region. The transition energy of a strained InGaN QW is smaller than that of bulk or strain-free InGaN material, which is attributed to the electron band bending in the QW by the field. By applying a forward bias, the transition energy increases. This leads to the blue-shift in EL because the current density increases due to partial screening of the QCSE by the injected carriers. The 450-nm peak does not show an obvious blue-shift but the monitor 470 nm-peaks are blue-shifted by 1.4 nm, 3.3 nm, and 7.6 nm for samples A, B, and C, respectively. These results show that the closer to the quantum confined stark effect the monitor 470 nm-emitting QWs is, the larger the blue-shift is. This phenomenon can be explained by the strain distribution due to the mismatch between MQWs and the EBL. The strain in QWs decreases as it moves from the p-region to n-region.

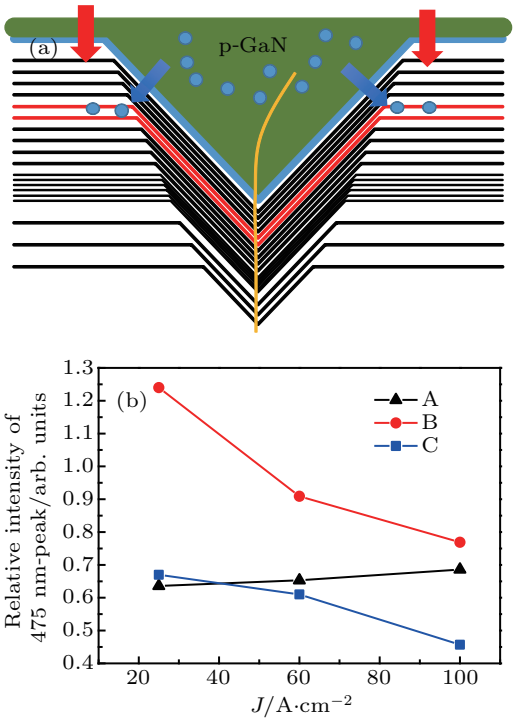


Fig. 4. (a) Schematic diagram for side-wall (blue arrow) and *c*-axis direction (red arrow) injection of holes, (b) plots of relative intensity of 475 nm *versus* current density for samples A, B, and C.

As the 475-nm QWs absorb the 450-nm emission from around the 450-nm QWs, the intensity of 475-nm emission peaks includes two parts: the first is from the recombination of injected electron and holes, and the second is due to excitation by the 450-nm emission from other QWs. To eliminate PL excitation by 450-nm emissions, samples D, E, and F with only monitor DQWs as shown in Fig. 1(b), are characterized under different current densities. Figure 6 shows the external quantum efficiency (EQE) and forward voltage (V_f) for samples D, E, and F as a function of driving current density. In the whole range of measurement current density, the V_f of sample E is 0.15 V–0.2 V lower than that of samples D and F. The lower V_f for sample E suggests that the holes are injected though side-wall preferentially into the 5th and 6th c-plane QWs, *i.e.*, the middle two QWs of sample B. The higher V_f for sample F is possibly due to the hole injection along the *c* axis with a large distance shown in Fig. 4(a) by red arrows, and the higher V_f for sample D can be attributed to the sharp apex of V-pits leading to a crowding of hole transportation, or the thicker cover layers on the side-wall resulting in a large transportation distance. At a current density of 25 A/cm^2, the EQE of sample E is $\sim$ 61.1%, which is higher than that of sample D ($\sim$ 54.7%) and F ($\sim$ 38.1%). This can be attributed to the fact that the holes are mainly distributed in the middle portion of the MQW active region leading to a high radiative recombination rate of electron-hole pairs, resulting in the same conclusion reached for samples A, B, and C.

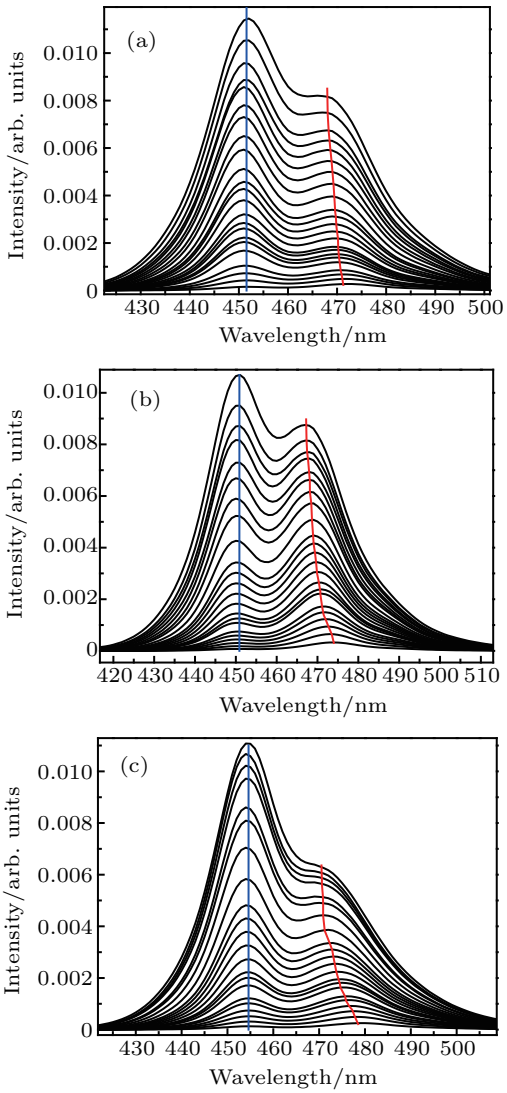


Fig. 5. EL spectra of (a) sample A, (b) sample B, and (c) sample C for driving current density ranging from 0.3 A/cm^2 to 100 A/cm^2.

The EQE and V_f of sample E are always the best in a range from 0.3 A/cm^2 to 150 A/cm^2, which can be taken as an effective method to optimize a proper size of V-pits to obtain the best performance. Here, the droop is defined as $(\eta_{\text{peak}} - \eta_{\text{test current}})/\eta_{\text{peak}}$, where η is the EQE. The effi-

ciency droop of sample E at 60 A/cm^2 is 28.9%, which is 27% and 8% lower than that of sample D (39.7%) and sample F (31.4%), respectively. The excellent performance of sample E is attributed to the side-wall injection of holes into the middle region of MQWs, as discussed in Fig. 4(a). However, when the driving current density increases further to 160 A/cm^2, the efficiency droop of sample E goes up to 61.4%, which is similar to that of sample D (60.6%) and sample F (60.7%). The reason for this is that under a higher current density, the efficiency droop effect mainly results from the inadequate holes due to the inefficient Mg doping, and the aggravated overflow of electrons to the p-region.[5] It is noted that the maximum EQE for samples E and F are achieved at a driving current density of $\sim$ 2 A/cm^2. Meanwhile, the EQE for sample D decreases from very low current density, with a low EQE value compared with that for samples E and F in the whole test current density. This phenomenon is a consequence of the serious overflow of electrons from the QW by the n-GaN layer, *i.e.*, the bottom of the MQW region. In the range of 25 A/cm^2–100 A/cm^2, the EQE curve of sample D presents a relatively flat trend compared with that of samples E and F, which is the reason for the slight increase of the relative EL intensity of 475-nm emission of sample A, as shown in Fig. 4(b). The large V-pits in our samples give rise to the preferential injection of holes into the middle part of MQW active region, leading to a lower V_f, higher EQE, and lower efficiency droop, which are greatly beneficial for high-power III–nitride LEDs.

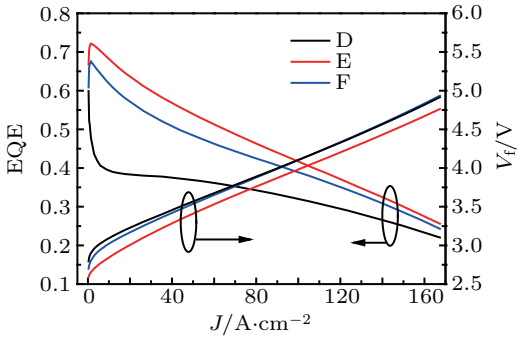


Fig. 6. Plots of EQE and V_f for samples D, E, and F *versus* injection current density for samples D, E, and F.

4. Conclusions

In this work, the efficiency droop of III–nitride LEDs with large V-pits is investigated by using specifically designed structures. The stronger EL emission of sample B and lower V_f of sample E indicate the higher hole density in the QWs in the center of the MQW active region. This suggests that large V-pits lead to a side-wall injection of holes into the *c*-plane QWs at the center region of MQWs, which gives rise to a reduced efficiency droop of 28.9%, at least 8% lower than that of other samples at 60 A/cm^2. The modified distribution of holes in MQWs makes III–nitride LEDs with large V-pits perform reasonably better in high-power applications in the SSL market.

References

[1] Schubert E F and Kim J K 2005 *Science* **308** 1274
[2] Krames M R, Shchekin O B, Mueller-Mach R, Mueller G O, Zhou L, Harbers G and Craford M G 2007 *J. Disp. Technol.* **3** 160
[3] Tan C K , Zhang J, Li X H , Liu G, Tayo B O and Tansu N 2013 *J. Disp. Technol.* **9** 272
[4] Yan Q X, Zhang S F, Long X M, Luo H J, Wu F, Fang L, Wei D P and Liao M Y 2016 *Chin. Phys. Lett.* **33** 078501
[5] Verzellesi G, Saguatti D, Meneghini M, Bertazzi F, Goano M, Meneghesso G and Zanoni E 2013 *J. Appl. Phys.* **114** 071101
[6] Akyol F, Nath D, Krishnamoorthy S, Park P and Rajan S 2012 *Appl. Phys. Lett.* **100** 111118
[7] Xu J, Schubert M F, Zhu D, Cho J, Schubert E F, Shim H and Sone C 2011 *Appl. Phys. Lett.* **99** 041105
[8] Park J H, Yeong Kim D, Hwang S, Meyaard D, Fred Schubert E, Dae Han Y, Won Choi J, Cho J and Kyu Kim J 2013 *Appl. Phys. Lett.* **103** 061104
[9] Chang C Y, Li H, Shih Y T and Lu T C 2015 *Appl. Phys. Lett.* **106** 091104
[10] Nakamura S 1998 *Science* **281** 956
[11] Yakimov E B 2016 *Jpn. J. Appl. Phys.* **55** 05FH04
[12] Hangleiter A, Hitzel F, Netzel C, Fuhrmann D, Rossow U, Ade G and Hinze P 2005 *Phys. Rev. Lett.* **95** 127402
[13] Okada N, Kashihara H, Sugimoto K, Yamada Y and Tadatomo K 2015 *J. Appl. Phys.* **117** 025708
[14] Sheen M H, Kim S D, Lee J H, Shim J I and Kim Y W 2015 *J. Electron. Mater.* **44** 4134
[15] Kim J, Kim J, Tak Y, Chae S, Kim J Y and Park Y 2013 *IEEE Electron Dev. Lett.* **34** 1409
[16] Le L, Zhao D, Jiang D, Li L, Wu L, Chen P, Liu Z, Li Z, Fan Y and Zhu J 2012 *Appl. Phys. Lett.* **101** 252110
[17] Quan Z, Wang L, Zheng C, Liu J and Jiang F 2014 *J. Appl. Phys.* **116** 183107
[18] Kim J, Cho Y H, Ko D S, Li X S, Won J Y, Lee E, Park S H, Kim J Y and Kim S 2014 *Opt. Express* **22** A857
[19] Li Y, Yun F, Su X, Liu S, Ding W and Hou X 2014 *J. Appl. Phys.* **116** 123101
[20] Kumakura K, Makimoto T, Kobayashi N, Hashizume T, Fukui T and Hasegawa H 2005 *Appl. Phys. Lett.* **86** 052105
[21] Ryou J H, Yoder P D, Liu J, Lochner Z, Kim H, Choi S, Kim H J and Dupuis R D 2009 *IEEE J. Sel. Top. Quantum Electron.* **15** 1080